Modeling and Experimental Studies of Emulsion Copolymerization Systems. I. Experimental Results

ODAIR ARAUJO,[1] REINALDO GIUDICI,[2] ENRIQUE SALDÍVAR,[3] W. HARMON RAY[4]

[1] Rhodia S. A., Departamento de Processos, Usina Química de Paulínia, 13140-000, SP, Brasil

[2] Departamento de Engenharia Química, Escola Politécnica, Universidade de São Paulo, 05424-970, SP, Brasil

[3] CID-GIRSA Corporativo S. A. de C. V., Lerma, Edo de México, 52000, México

[4] Department of Chemical Engineering, University of Wisconsin, Madison, Wisconsin 53706, USA

Received 27 December 1999; accepted 31 May 2000

ABSTRACT: A systematic experimental and modeling study of several emulsion copolymerization systems has been performed, and will be reported in a series of papers. Ten binary and three ternary copolymerizations involving styrene, methyl methacrylate, butyl acrylate, butadiene, vinyl acetate, acrylic acid, and ethylene were studied varying polymerization temperature, monomer composition, water to monomer ratio, initiator and emulsifier concentrations. Conversion, particle size, copolymer composition, and gel content were measured at several reaction times. The goal of this series of papers is to assess our quantitative understanding of emulsion copolymerization expressed in the form of a comprehensive mathematical model applied to monomers widely used in industry. In this first paper of the series, a global comparison of the experimental results is made. It is observed that the gel content is higher in systems containing butyl acrylate and butadiene, and smaller in systems containing methyl methacrylate. Larger particle numbers are obtained for lattices containing acrylic acid and butadiene. It is also shown that, for most of the systems, integration of the simple Mayo–Lewis equation is adequate to explain the drift in copolymer composition observed experimentally. © 2001 John Wiley & Sons, Inc. J Appl Polym Sci 79: 2360–2379, 2001

Key words: emulsion copolymerization; mathematical modeling; experimental

INTRODUCTION

The importance of the emulsion polymerization process has grown dramatically since World War II mainly because of the need of water-based latexes to be used as coatings and adhesives. Recently, an increase in environmental awareness has led to the replacement of processes that use solvents by cleaner water-based emulsion polymerization processes. In order to improve the product performance, the recipes and processes have become more complex introducing, for instance, multicomponent polymerization and copolymerizable emulsifiers. Also, there is a need for reducing the levels of residual monomer in the products and for increasing the productivity of the processes. As the complexity increases, better

Correspondence to: Enrique Saldívar (esaldiva@mail.girsa.com.mx).

Contract grant sponsor: CNPq.
Contract grant sponsor: FAPESP.
Contract grant sponsor: Rhodia.
Contract grant sponsor: CID-GIRSA.
Contract grant sponsor: UWPREL.

Journal of Applied Polymer Science, Vol. 79, 2360–2379 (2001)

Table I Copolymerization Systems Studied and Their Reactivity Ratios[7]

System	Code	r_1	r_2
Styrene/Methyl Methacrylate	S/M	0.45	0.47
Styrene/Butadiene	S/B	0.64	1.38
Styrene/Butyl Acrylate	S/BA	0.8	0.15
Styrene/Acrylic Acid	S/AA	0.15	0.25
Methyl Methacrylate/Butyl Acrylate	M/BA	1.5	0.3
Methyl Methacrylate/Vinyl Acetate	M/VA	22.21	0.07
Methyl Methacrylate/Acrylic Acid	M/AA	1.25	0.23
Methyl Methacrylate/Butadiene	M/B	0.7	0.32
Vinyl Acetate/Butyl Acrylate	VA/BA	0.02	3.48
Vinyl Acetate/Ethylene	VA/E	1.5	0.74

process understanding through experiments and mathematical modeling have gained importance in the development of new technologies and recipes.

The structure of the chain has a profound influence in the physical properties of the final product. The polymer chain structure and composition can be explained by the kinetic scheme and thermodynamic equilibrium equations. Mayo and Lewis[1] and others studied the determining factors for the copolymerization case, and assumed that the reaction rate depends on the free radical terminal identity and does not depend on the identity of the penultimate monomer in the chain. This theory is called terminal or Markov first order model. More recently, Ma et al.,[3] Fukuda et al.,[4] and others, by measuring independently the rate coefficients for propagation and termination in free-radical copolymerization, have found experimental evidence to support the theory that the penultimate model is more appropriate to explain the polymer composition and rate of reaction in some free-radical copolymerization systems. Thus more complex kinetic modeling of propagation in copolymerization may remove the necessity for additional parameters associated with the termination mechanism (e.g., ϕ factor[5]).

Although there is no complete understanding of the free-radical kinetics of copolymerization and of some of the phenomena present in *ab initio* polymerizations in emulsion (e.g., nucleation of particles), there is a considerable body of information that allows us to have a semiquantitative understanding of emulsion copolymerization. However, despite the industrial importance of this type of processes, there have been very few systematic studies of a general nature[6] that include a number of copolymerization systems and focus on the effect of operational variables on the process and on polymer properties. Previous efforts have been concentrated on specific systems, lacking the perspective necessary to establish what parts of the general theory for emulsion copolymerization are fairly well established and which ones require additional research effort. The main goal of this work is to contribute to a better understanding of the emulsion copolymerization process from a general perspective. This is better achieved by using experiments and comparison with a comprehensive mathematical model that includes generally accepted pictures of the different phenomena and mechanisms that comprise the emulsion copolymerization process. The experiments were designed in such a way that they provide a systematic comparison of different comonomer systems, in order to point out which general areas of these systems are understood and which ones need more research.

The copolymerization systems selected for study are presented in Table I. They cover a wide range of monomer solubilities in water (Table II) and also a wide range of copolymerization behavior that can be predicted. In Figure 1 several copolymer pairs are shown as a function of reac-

Table II Solubilities in Water (taken from Ref. 8)

Monomer	Solubility in Water
Acrylic acid	Total
Butadiene	0.081% (25°C)
Butyl acrylate	0.16% (25°C)
Ethylene	0.9% (80°C, 4500psig)
Methyl methacrylate	1.59% (20°C)
Styrene	0.027% (25°C)
Vinyl acetate	2.4% (20°C)

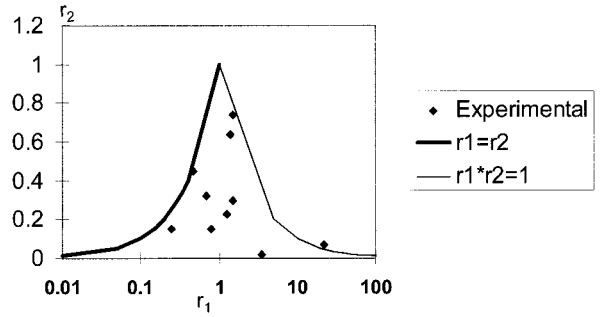

Figure 1 Reactivity ratios for the systems studied.

tivity ratios r_1 and r_2. This graphic is useful to visualize the copolymerization behavior.

In addition to the ten copolymerization systems presented in Table I, we also studied the following terpolymerizations:

—Styrene/Butadiene/Methyl Methacrylate (S/B/M)

—Styrene/Methyl Methacrylate/Butyl Acrylate (S/M/BA)

—Styrene/Butadiene/Acrylic Acid (S/B/AA)

—Methyl Methacrylate/Vinyl Acetate/Butyl Acrylate (M/VA/BA)

In this paper, which is the first one of a series taking a general approach to study emulsion copolymerization, we describe general aspects and results of the experimental studies. Future papers will be dedicated to a comparison of experimental results and model simulations for styrenic and acrylic binary copolymer systems, as well as terpolymerization systems. We have divided the different systems in three sets for presentation and organizational purposes, but the theory represented by the mathematical model that will be used for analysis[9] gives a unified view of our understanding of emulsion copolymerization.

The organization of this paper is as follows. In the next section we describe the experimental equipment and techniques used for the emulsion copolymerization reactions and the polymer characterization. The experimental design used is also discussed. Then, overall experimental results and comparisons are presented and discussed, and finally, conclusions are drawn.

EXPERIMENTAL

Reagents and Reagent Purification

All reagents used in this work were of Aldrich quality/grade. Most of the monomers were purified to extract inhibitor. Styrene (99%, Aldrich No. S-497-2) was washed several times with a 10% sodium hydroxide solution until the extract did not present color. The inhibitors were extracted from the monomers vinyl acetate (99% Aldrich No. V-150-3), methyl methacrylate (99% Aldrich No. M5590-9), and butyl acrylate (99% Aldrich No. 23492-3) using inhibitor extraction columns (Aldrich No. 30631-2). Butadiene monomer (99.5% Matheson, instrument purity, less than 0.05% air in vapor phase) was distilled at ambient temperature and condensed at dry ice temperature. Ethylene (polymer grade, 99.9% minimum) and acrylic acid (Aldrich) monomers were used as received without purification.

The initiator was ammonium persulfate (98% Aldrich No. 24861-4), kept under refrigeration. The emulsifier employed was sodium dodecyl sulfate (98% Aldrich No. 86201-0). The chain transfer agents used for the system B/S/M were *tert*-dodecyl mercaptan (Aldrich No. 16915-3) and hexyl mercaptan (Aldrich No. 23419-2). Deionized water was used throughout all the experimental work. Initiator, emulsifier, and chain transfer agents were used as received without further purification.

Nitrogen sparging was used to remove oxygen from the reaction mixture and from the reactor since oxygen is a highly reactive inhibitor that is usually dissolved in the reactants.

Polymerization Method

Polymerizations were carried out in a jacketed 2.4-L stainless steel (304) batch reactor. The four-blade turbine agitator is magnetically moved with a rotation speed in the range from 0 to 1000 rpm. The temperature was controlled within ± 0.5°C using a PID controller.

All polymerizations were carried out with the reactor closed, without external condenser. For safety reasons, the reactor is equipped with a rupture disk and a relief valve and vent. Maximum pressure allowed is 1000 psi.

There are six feedlines and pumps for liquid reagents. However, in this work, all polymerizations were carried out in batch mode. The exception were the runs involving ethylene as comonomer, in which the gas was continuously fed. The ethylene consumption rate was measured by a high precision balance (150 kg $\pm$ 0,1 g) the cylinder was placed upon.

Polymerization proceeded by first charging the water and the emulsifier. After dissolution of the emulsifier, the monomers were charged into the

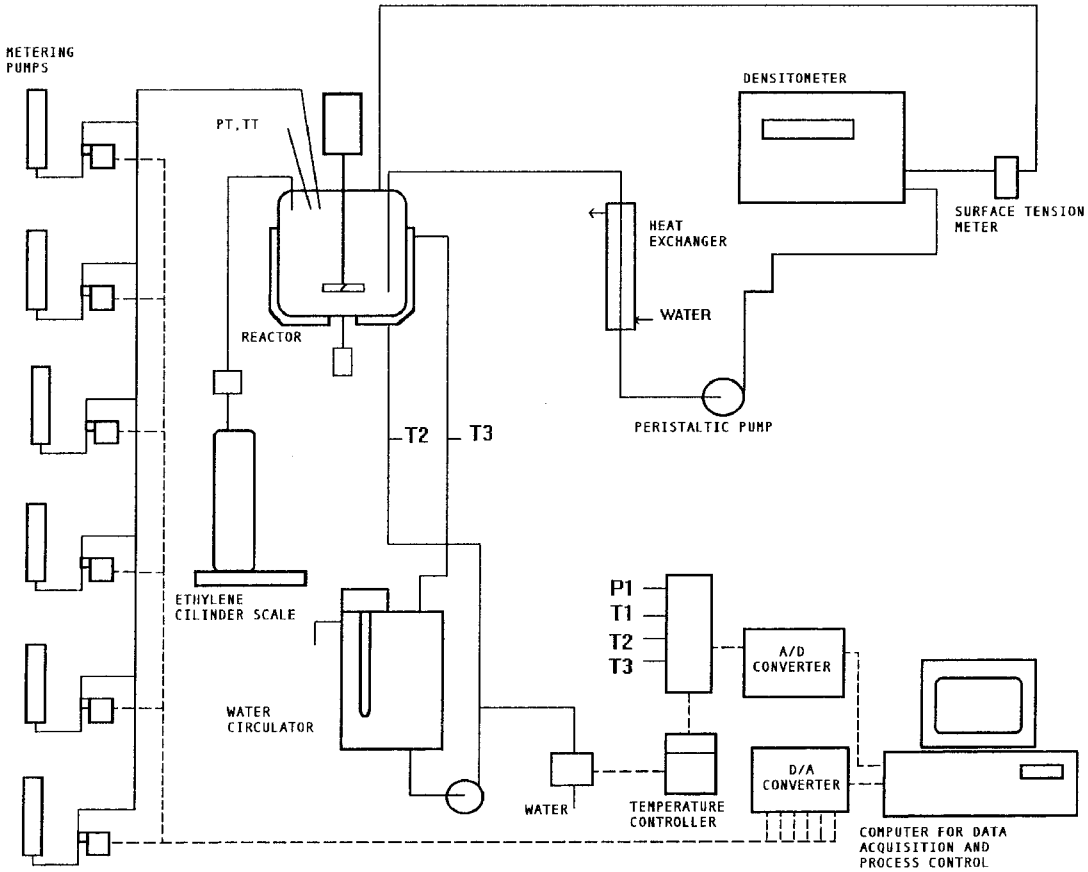

Figure 2 Schematic diagram of the equipment.

reactor. The reactor was then closed, the agitation was started and the reactor was sparged with nitrogen for about 10 min to deoxygenate the mixture; then the heating was started. When the reactor contents reached the desired temperature, the initiator solution was charged. This point was considered zero reaction time. Samples were taken from the reactor at various time intervals for analysis.

In the runs with low pressure (up to 10 psi), the samples for gravimetric analysis were taken from the reactor directly through the valve at the bottom of the reactor. For pressures higher than 10 psi, a system with valves and a 10-cm^3 stainless steel cylinder was connected to the valve at the bottom of the reactor. After taking the sample, the cylinder was depressurized in a hood and the sample was collected.

A general schematic view of the experimental apparatus is shown in Figure 2.

Product Characterization

The importance of experimental studies of polymerization kinetics with complete data information content has been discussed by Penlidis.[10] In order to test our quantitative undestanding of emulsion polymerization, we have tried to obtain extensive information from each experiment. Thus, the following measurements have been taken: reactor pressure, total conversion (by gravimetry), particle size (by dynamic laser light scattering), polymer composition (by proton NMR spectroscopy), and gel fraction (by filtration), all of them along the course of the polymerization.

Total Conversion via Gravimetric Analysis

The samples taken from the reactor were placed into preweighed 20-mL aluminum dishes, and short-stopped with about 1 mL of a 3% hydroquinone solution. The dish was weighed and dried to a constant weight, first at ambient temperature for 24 h and then at 50°C in an oven under vacuum. The total conversion was calculated by

$$x = \frac{\left(\frac{m_{AS} - m_p - 0.03m_{SH}}{m_A - m_p - m_{SH}}\right)M_{TR} - M_E - M_I}{M_M} \quad (1)$$

where m_{AS} is the weight of dish and dry sample, m_p is the weight of the empty dish, m_{SH} is the weight of hydroquinone solution added to the sample, and M_{TR}, M_E, M_I, and M_M are the weight of the reactor contents, emulsifier, initiator, and monomers in the initial charge to the reactor.

The standard deviation of the conversion was estimated to be 0.003 for an average value of 0.995 using 17 repeated samples taken at the end of the same run.

Particle Size

Particle size of the latexes were measured using dynamic laser light scattering equipment (Malvern 4700). The measurements were done at 25°C using a scattering angle of 90°. Samples of about 9 cm^3 were collected in glass tubes containing 1 cm^3 of a 3% hydroquinone solution, 1 cm^3 of particle stabilizer Triton X-100 (Aldrich # 23472-9), and 8 cm^3 of deionized water. Further dilution with water was done when the sample is placed in the measurement cell in order to adjust the concentration of particles in the range required by the equipment. The results here reported represent the *z*-average particle diameter, for which the standard deviation of the measurement was estimated to be 2 nm.

Copolymer Composition

The samples of dry polymer from the conversion analysis were used to measure the polymer composition by proton nuclear magnetic resonance (^{1}H NMR). The samples were prepared by preparing solutions of 0.1% of dry polymer in deuterated chloroform (98%, Aldrich No. 23689-6). The spectra analysis and the calculation of the relative amounts of monomer bound in the polymer were performed at the Chemistry Department of the University of Wisconsin using a 300 MHz NMR equipment from Bruker.

Glass Transition Temperature

Samples of dry polymer from the conversion analysis were also used to measure the glass transition temperature. Two different techniques were used: differential scanning calorimetry (DSC) and dynamic mechanical analysis (DMA). The DSC analysis was carried out in a differential scanning calorimeter Netzsch model DSC 200, in a temperature range of −150 to +150°C, with a heating rate of 10°K/min, a nitrogen purge flow rate of 25 cm^3/min, protection nitrogen flow rate of 300 cm^3/min. The samples that did not present good resolution by DSC were analyzed via DMA.

Gel Content

The amount of polymer retained in the filter during the preparation for GPC analysis was dried and weighed. The amount of this residue may give an estimate of gel content in the polymer. While this is a simplified measurement of gel, this shortcut technique provides qualitative (or at best "semiquantitative") data of gel content. Therefore, these results may be used only for comparative rather than quantitative analysis.

Pressure

In each run the pressure in the reactor was measured during the polymerization. Pressure measurements are useful to identify some changes in the polymerization, such as the instant in which the monomer droplets disappear, relating the pressure to the conversion. The sensitivity of the pressure–conversion relationship is higher for more volatile monomers (e.g., butadiene). When the reactor operates closed, without external condenser, as in this case, the combination of temperature and pressure measurements, along with thermodynamic equilibrium calculations may be used to infer conversion.

Experimental Design

The objective of the experiments was to obtain reliable data that may serve for model validation and to improve our understanding of emulsion copolymerization. In addition, the data may indicate which factors and interactions are most significant, and eventually they may reveal new behavior not previously considered or explained.

The design of experiments provides a valuable tool for choosing the "best" experimental conditions, especially in the cases of complex systems with multiple factors involved like emulsion copolymerization and terpolymerization. In this sense a good experimental design can be useful to reduce the number of experiments required to obtain a given information, specially when many factors are under study.

In the present work, the following five factors were studied: temperature (T), initiator initial concentration (I) , emulsifier initial concentration (E), total monomer concentration (M_T), and molar ratio between the comonomers (A/B). Their effects were studied for each one of the systems consid-

ered (ten copolymerization and four terpolymerization systems).

The approach taken to define our experiments can be seen as a mixed design. We started the experiments according to a fractional factorial design.[11] In addition, further experiments were chosen to augment the resolution of individual variables and pairs of variables effects (two-by-two grouping), in order to obtain a better appreciation of effects. The resulting map of the final design is shown in Table III, in which the shaded positions indicate the runs effectively performed. Table III may be examined either along the rows (i.e., comparing different systems under the same conditions) or along the columns (i.e., analyzing the effects on a given copolymerization system).

In this article we restrict ourselves to the analysis and comparison of the different systems, thus following the "row" approach. Subsequent papers in this series will follow the "column" approach, focusing the interpretation of the results within the framework of a mathematical model.

RESULTS AND DISCUSSION

The experiments were planned in order to evaluate the effect of operational conditions on the development of the particle mean diameter, number of particles, monomer conversion, polymerization rate, and copolymer composition. In addition, glass transition temperature and gel content were measured in the final polymer.

In this section, comparative results among the different copolymers and terpolymers are presented. Reliable comparison is possible since runs were carried out under similar conditions, so that other undesirable factors (such as operation and analytical procedures, quantities and quality of the reactants) do not mask the comparison.

Number of Particles

The particle concentration N_p (number of particles per cm^3 of water) was estimated by using

$$N_p = \frac{6M_T x_m}{\rho_p \pi d_p^3} \tag{2}$$

where M_T is the initial total monomer concentration (g/cm^3 of water) ρ_p is the polymer density (g/cm^3), d_p is the average particle diameter (cm), and x_m is the total weight conversion. This formula assumes that the particles contain only polymer, which is consistent with the measurement of particle size made using a very diluted sample, presumably corresponding to the diameter of unswollen particles. The value of polymer density was assumed to be 1.1 g/cm^3, although a more proper value would be an average of the density of the correspondent homopolymers; the effect of this simplification, however, is within the standard deviation of particle diameter measurements.

The variation of the number of particles with conversion allows one to identify the extension of the nucleation period (increase of N_p with time or conversion) and the occurrence of flocculation (decrease of N_p).

Figure 3 shows the average values, standard deviations, and maximum and minimum values of the particle concentration at the end of the polymerization for the different systems studied. Particle concentrations ranged from 5×10^{14} to 6×10^{15} particles/cm^3 of water.

The aggregation number for the sodium dodecyl sulfate is about 80 molecules/micelle and its critical micellar concentration is about 0.0081 mol/L.[12] Using these values and the emulsifier concentrations (4 and 8 g/L) used in the experiments, the micelle concentration would range from 4×10^{16} to 1.5×10^{17} micelles/cm^3 of water. These figures are higher than the experimentally observed particle concentration, showing that not all the initial micelles are nucleated. This is due to the fact that as soon as new particles are nucleated and start growing, emulsifier molecules from the remaining micelles are used to cover the surface of the growing particles.

Among all the systems studied, the terpolymer S/B/AA presented the highest number of particles. Except for the last four systems shown in Figure 3 (S/B/AA, B/M, S/AA, and B/S/M), all the remaining systems presented almost the same particle concentration. It is interesting to note that systems with acrylic acid presented higher particle concentrations. Acrylic acid, the most hydrophilic monomer used in this work, will favor particle formation by homogeneous nucleation. The results show that AA promotes particle formation when it polymerizes with a low solubility monomer.

Particle diameter curves are plotted in Figures 4 for copolymers with styrene and in Figures 5 for copolymers with methyl methacrylate. Figure 4(a) shows that the particle diameter for the system S/B 70%/30% is higher than for the other

Table III Map of the Experiments

	T	I	E	MT	A/B	A= S	S	S	S	M	M	M	M	VA	S	S	S	M
						B= M	B	BA	AA	BA	VA	AA	B	BA	B	M	B	VA
															M	B	AA	BA
1	+	+	+	+	+													
2	+	+	+	+	-													
3	+	+	+	-	+													
4	+	+	+	-	-													
5	+	+	-	+	+													
6	+	+	-	+	-													
7	+	+	-	-	+													
8	+	+	-	-	-													
9	+	-	+	-	+													
10	+	-	-	+	+													
11	+	-	-	-	+													
12	+	-	-	-	-													
13	-	+	+	+	+													
14	-	+	+	-	+													
15	-	+	+	-	-													
16	-	+	-	-	+													
17	-	+	-	-	-													
18	-	-	+	+	-													
19	-	-	+	-	+													
20	-	-	+	-	-													
21	-	-	-	+	+													
22	-	-	-	-	+													
23	-	-	-	-	-													
24	+ +	-	+	-	-													
25	+ +	-	-	-	+													
26	+ +	-	-	-	-													
27	+	+	+	-	+ +													
28	+	-	-	-	+ +													
29	-	+	-	-	+ +													
30	-	-	+	-	+ +													
31	-	-	-	-	+ +													

	-	+	+ +
T = temperature (C)	60	70	80
I = initiator concentration, g/l/H2O	0,45	0,90	
E = emulsifier concentration, g/l H2O	4	8	
MT = total monomer concentration g/cm3 H2O	0,34	0,55	
A/B = molar ratio between the monomers	0,30	0,70	0,95

systems. This effect, however, is not observed in the case S/B 30%/70%, as shown in Figure 4(b). Additional evidence of this interesting behavior was also found in the experiments with the system S/B/M, in which particle size was higher for recipes rich in S than for the systems rich in B or M.[13]

The system S/AA presented the lowest particle diameter, about 50 nm. Acrylic acid, as already mentioned, can promote the increase in the number of particles by homogeneous nucleation, due to its high solubility in water. It can also work under some conditions as surfactant. Due to the larger number of particles formed, they will grow smaller at comparable amounts of surfactant.

Figures 5(a) and 5(b) show that the system butadiene/methyl methacrylate presents lower particle diameter (therefore higher number of particles) than the other systems, as opposed to what is observed in Figure 4(a) for the system styrene/butadiene. It seems that butadiene in the presence of a less hydrophobic comonomer like M may promote the formation of more particles. This may be due to the slow initiation observed for butadiene emulsion homopolymerization,[14] compounded with a relatively increased importance of the homogeneous nucleation. In general, an increased content of butadiene seems to increase the number of particles, even for the system S/B, but the effect is more pronounced for less hydrophobic comonomers.

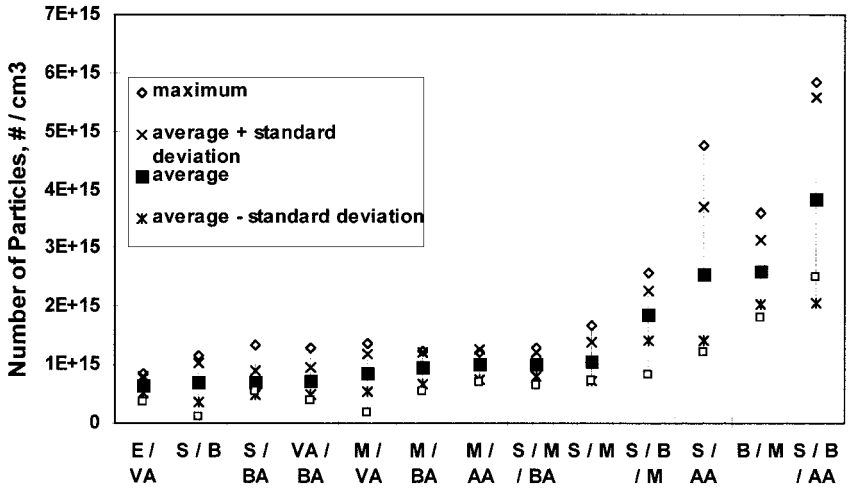

Figure 3 Average values, standard deviations, and maximum and minimum values of the particle concentration at the end of the polymerization for the different systems studied.

Figure 6 shows the behavior of N_p with the fractional mass conversion x_m, for copolymerization runs with 70% styrene and 30% of the other comonomer. Particle concentration tends to become almost constant after a given conversion, except for the system styrene/acrylic acid. In these systems with 70% styrene (that has low solubility in water), the final particle concentration can be correlated to the comonomer solubility, as long as more soluble comonomers produced higher number of particles. This result indicates the effect of comonomer solubility on particle nucleation.

However, the same behavior is not seen in Figure 7 for systems with 70% of MMA (a moderately soluble monomer). In this case the solubility of the comonomer does not seem to play the main role in particle nucleation. It is interesting to note that the system 70% MMA/30% butadiene presented the highest number of particles.

Polymerization Rate

The maximum polymerization rate was obtained for each run by evaluating the maximum slope in the conversion vs time curve.

The values of maximum polymerization rate for several systems are shown in Figure 8. All systems with butadiene presented the lowest polymerization rates, specially for cases containing styrene. The system that presented the highest rate was methyl methacrylate/acrylic acid. Therefore, it seems that there exists a correlation between monomer solubility in water and polymerization rates, maybe due to the relative increase of homogeneous nucleation in these systems and its contribution toward a larger number of particles.

Figures 9 and 10 show the conversion vs time curves for the copolymers of S. For the systems with comonomers M, BA, and AA, the polymerization rates are of the same magnitude, while for the system styrene/butadiene the polymerization rate is comparatively much lower. The rate decreases in the sequence S/AA $>$ S/BA = S/M $\gg$ S/B. Whether this is due to an inherent low rate constant for the homopolymerization of butadiene, or to a mechanism (e.g., desorption) that eliminates radicals from the particles in the presence of butadiene, as argued by Weerts et al.,[14] is still a matter of debate.

The conversion vs time curves for the copolymers of methyl methacrylate are presented in Figures 11 and 12. Again, the system with butadiene comonomer presented lower polymerization rate than the systems with other comonomers. The rate decreases in the sequence M/AA $>$ M/BA $>$ M/S $\gg$ M/B.

An interesting feature of the system methyl methacrylate/vinyl acetate (M/VA) can be clearly seen in Figure 12. The conversion vs time curve for this system shows typically two periods. During the first period, up to 70% conversion for this run (70% M and 30% VAc), the process proceeded practically as an M homopolymerization. After the depletion of M, the remaining vinyl acetate

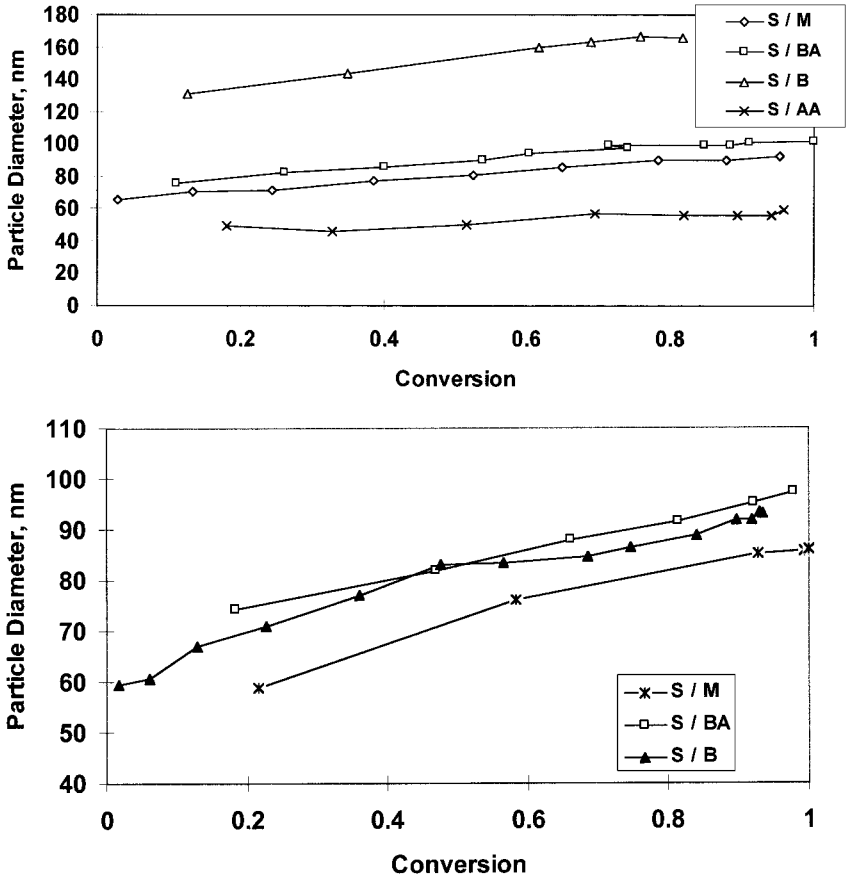

Figure 4 (a) Particle diameter for the systems S/B, S/M, S/BA, S/AA (70%/30%): T = 60°C, I = 0.45 g/L H_2O, E = 4 g/L H_2O, M_T = 0.34 g/cm^3 H_2O. (b) Particle diameter for the systems S/B, S/BA, S/M (30%/70%): T = 70°C, I = 0.45 g/L H_2O, E = 4 g/L H_2O, M_T = 0.34 g/cm^3 H_2O.

polymerizes in the second period. This behavior of "two consecutive homopolymerizations" was observed for all runs for this system, and the conversion in which the transition occurred was always closely related to the M content in the initial monomer mixture. This feature can be ascribed to the widely different reactivity ratios of the two comonomers, as discussed by Dubé and Penlidis[15] and Saldívar and Ray.[16]

Gel Content

The results presented in this section were used to verify, in a qualitative/comparative way, the intensity of the branching and crosslinking reactions in the different systems. However, since the gel content was measured by a simplified procedure, these results should not be used for quantitative modeling.

Figure 13 shows the gel content for each of the studied systems. The filtration of the polymers with acrylic acid were very troublesome, so that it was not possible to obtain even this simplified estimation of the gel content for these systems. Presumably the systems with acrylic acid lead to very high gel content. Therefore, the system S/AA was not included in Figure 13.

Systems with S and M did not present much gel, as their rate constants for chain transfer to polymer are very low. Monomers like V, E, and BA have significant chain transfer to polymer, and so will have gel. B, which has an extra double bond, can also form a network. Among the systems shown in Figure 13, those with BA presented the highest gel contents, followed by the systems with B. The main mechanism for branching and crosslinking in butadiene polymerization are the reactions with double bonds located on the

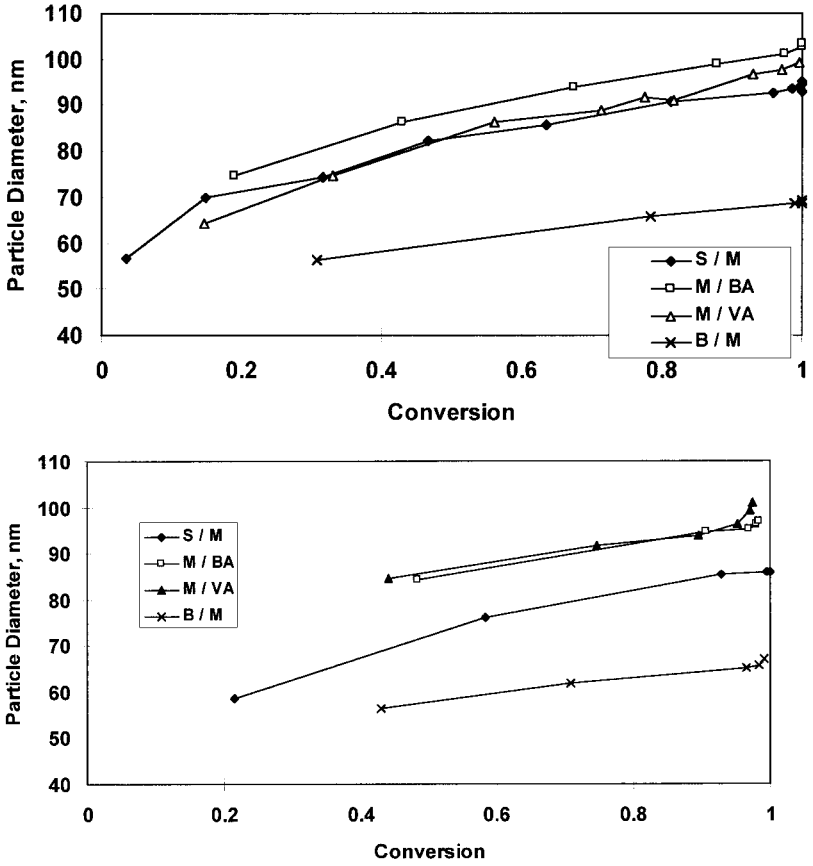

Figure 5 (a) Particle diameter for the systems S/M, M/BA, M/VA, B/M (70%/30%: T = 60°C, I = 0.45 g/L H_2O, E = 4 g/L H_2O, M_T = 0.34 g/cm^3 H_2O. (b) Particle diameter for the systems S/M, M/BA, M/VA, B/M (30%/70%): T = 70°C, I = 0.45 g/L H_2O, E = 4 g/L H_2O, M_T = 0.34 g/cm^3 H_2O.

polymer backbone (internal and/or pendant double bonds) and this mechanisms are well documented.[17,18] For the case of butyl acrylate, Dubé and Penlidis[15] also reported difficulties in filtering their emulsions for the analysis. In systems with butyl acrylate, gel formation may result from transfer to polymer and terminal double bond reactions.[19]

It is important to note that emulsion polymerization provides favorable conditions for branching and crosslinking reactions. Inside the particles, both polymer and free radical concentrations are high, so that both internal double bond reactions and transfer to polymer are much more likely to occur in emulsion than in solution polymerization.

Copolymer Composition

The classical treatment of copolymerization assumes that the reactivity of a propagating chain in a copolymerization is dependent only on the identity of the monomer unity at the growing end and independent of the chain composition preceding the last monomer unit.[17] This is the so-called first-order Markov or terminal model of copolymerization. In this model it is also assumed that the propagation reactions are irreversible, the propagation rate constants are independent of the chain length, and the chains are sufficiently large (long chain assumption). Also, monomer consumption in reactions other than propagation is considered negligible and the steady-state hypothesis is valid for each type of active species. Under these conditions, the following equation holds[17]:

$$\frac{d[M_1]}{d[M_2]} = \frac{[M_1](r_1[M_1] + [M_2])}{[M_2]([M_1] + r_2[M_2])} \tag{3}$$

where r_1 and r_2 are the reactivity ratios of monomer type 1 and monomer type 2, respectively, and

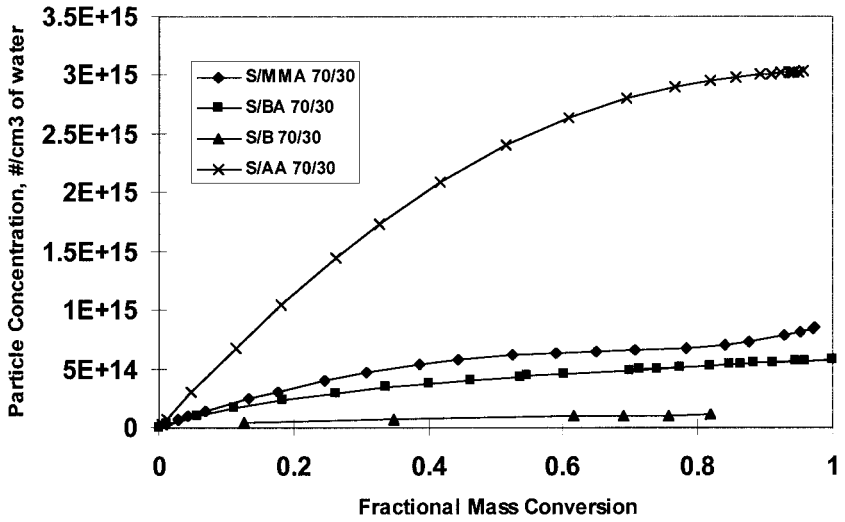

Figure 6 Particle number per cm^3 of water for the systems with 70 mol % of styrene in the initial monomer composition: T = 60°C, M_T = 0.34 g/g of water, E = 4 g/L of water, I = 0.45 g/L of water.

$[M_1]$ and $[M_2]$ are the monomer concentrations in the reaction medium. Equation (3) is the so-called copolymer composition equation, or Mayo–Lewis equation. In the case of emulsion polymerization, one must know the monomer concentration in the polymer particles, and this requires the use of thermodynamic equilibrium calculations.

As a first approximation, we have applied eq. (3) using total monomer concentrations instead of the concentrations into the particles. Therefore the mole fractions of monomer i in the monomer mixture in the particle (f_i) were first approximated by the total mole fractions of unreacted monomer i in the monomer mixture in the reactor f'_i. Considering this approximation, the copolymer composition equation can be written in terms of these variables as

$$\frac{df'_1}{dx} = \frac{f'_1 - F_1}{1 - x} \qquad f'_1(x = 0) = f'_{1,0} \tag{4}$$

$$F_1 = \frac{r_1(f'_1)^2 + f'_1 f'_2}{r_1(f'_1)^2 + 2f'_1 f'_2 + r_2(f'_2)^2} \tag{5}$$

$$f'_2 = 1 - f'_1 \tag{6}$$

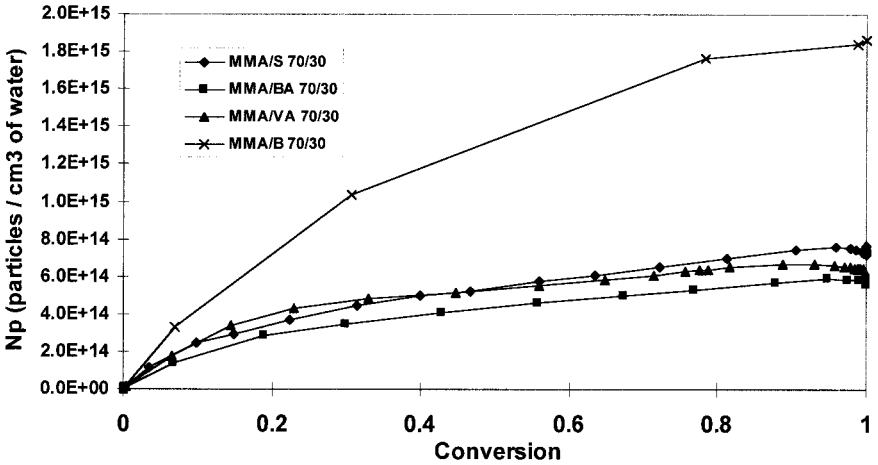

Figure 7 Particle number per cm^3 of water, for the systems with 70 mol % of methyl methacrylate in the initial monomer composition: T = 60°C, M_T = 0.34 g/g of water, E = 4 g/L of water, I = 0.45 g/L of water.

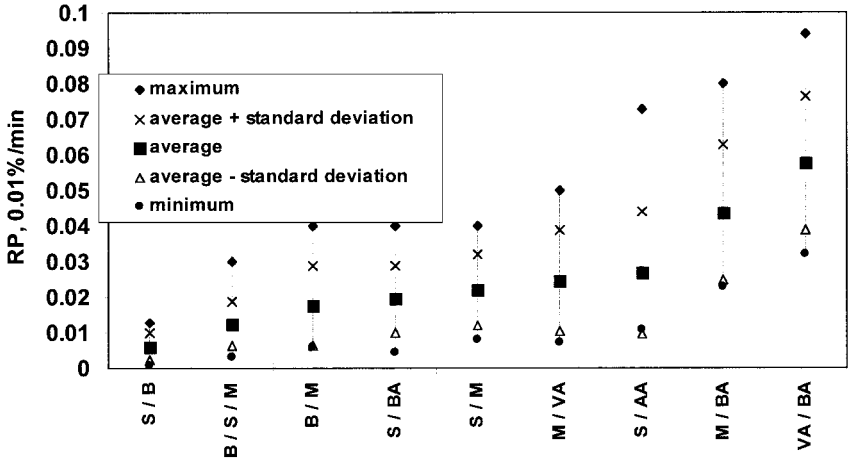

Figure 8 Maximum polymerization rate for the different studied systems.

Equation (4) was numerically solved by a marching technique with small increments in the total molar monomer conversion x. The values of the accumulated copolymer composition (mole fraction of monomer 1 in the polymer) were then obtained by

$$\bar{F}_1 = \frac{f'_{1,o} - f'_1(1-x)}{x} \tag{7}$$

The predictions from this simple approach are compared to the experimental data of copolymer composition measured by H^1 NMR spectroscopy. Reactivity ratios were taken from Brandrup and Immergut.[7]

Figures 14–19 show the comparison for two different initial monomer compositions (30 and 70 mol %). The simplified model is represented by the full curves in these figures. The concentrations of initiator ammonium persulfate (I), emulsifier sodium dodecyl sulfate (E), and M_T are indicated in each figure legend. It is interesting to see that good agreement was obtained for most of the systems studied, except for the pairs involving acrylic acid (Fig. 16) and, in lower proportion, for systems rich in vinyl acetate (Fig. 18). Comparatively higher deviations are observed in the systems with comonomers with more different water solubilities, especially in the cases with large amount of high water-soluble monomer. This suggests that the deviations could be in part ascribed to the higher solubility in water of these comonomers, causing some deviation when monomer partitioning is not considered.

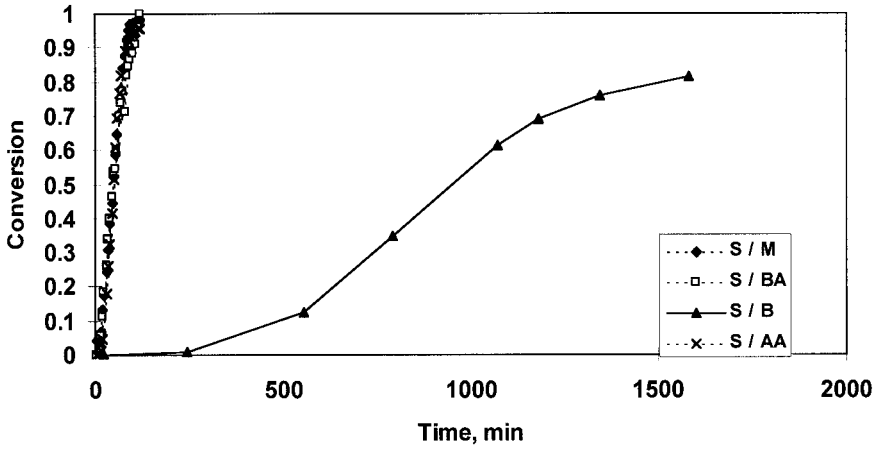

Figure 9 Conversion vs time curves for the copolymers of styrene S/M, S/B, S/BA, S/AA (70%/30%): T = 60°C, I = 0.45 g/L H_2O, E = 4 g/L H_2O, M_T = 0.34 g/cm^3 H_2O.

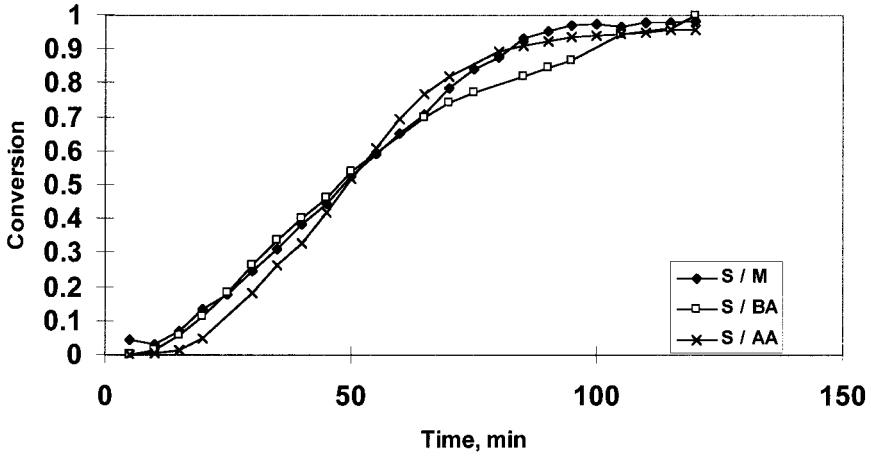

Figure 10 Conversion vs time curves for the copolymers of styrene S/M, S/BA, S/AA (70%/30%): T = 60°C, I = 0.45 g/L H_2O, E = 4 g/L H_2O, M_T = 0.34 g/cm^3 H_2O.

A second approach was made including thermodynamic equilibrium calculations along with the copolymer composition equation written for the monomer concentrations in the particles. This approach is expected to give more accurate results since the monomer partitioning is accounted for, so that the monomer concentration in the polymerization loci is used in the calculations by eq. (3). At each incremental step of total conversion in the copolymer equation, the partition model is solved to give the monomer concentration in each of the phases present (droplets, polymer particles, and aqueous phase). The monomer partition model used was based on the Morton extension of Flory–Huggins theory, as described by Gugliotta et al.[20] The numerical solution of the thermodynamic equilibrium model was obtained using the algorithm proposed by Armitage et al.[21] All parameters involved in the thermodynamic calculation were taken from the literature.

The predictions of this second approach are also shown in Figures 14, 15, and 17–19 as dashed curves. It is interesting to note that, in general, there is no important differences between the prediction of the simplified model that assumes global mole fractions and the predictions of the more accurate model that account for the monomer partitioning. The differences between the two approaches are, in most cases, lower than the expected experimental errors for measurements of copolymer composition. Since we need to consider only the ratio of partitioning coefficients to determine copolymer composition, then for monomers with low water solubilities, this ratio

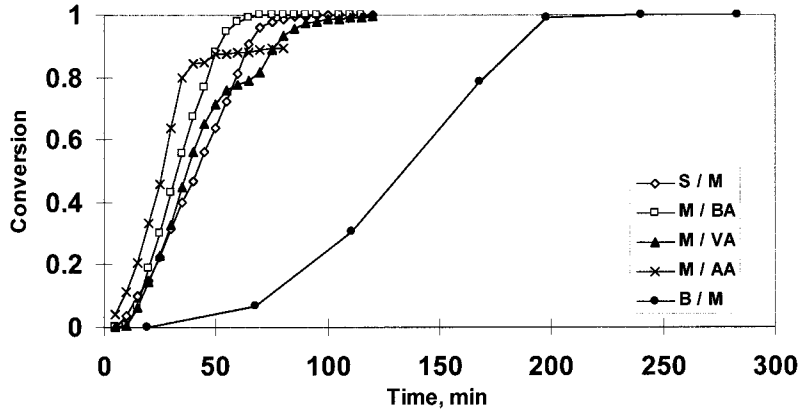

Figure 11 Conversion vs time curves for the copolymers of methyl methacrylate M/S, M/BA, M/AA, M/VA, M/B (70%/30%): T = 60° C, I = 0.45 g/L H_2O, E = 4 g/L H_2O, M_T = 0.34 g/cm^3 H_2O.

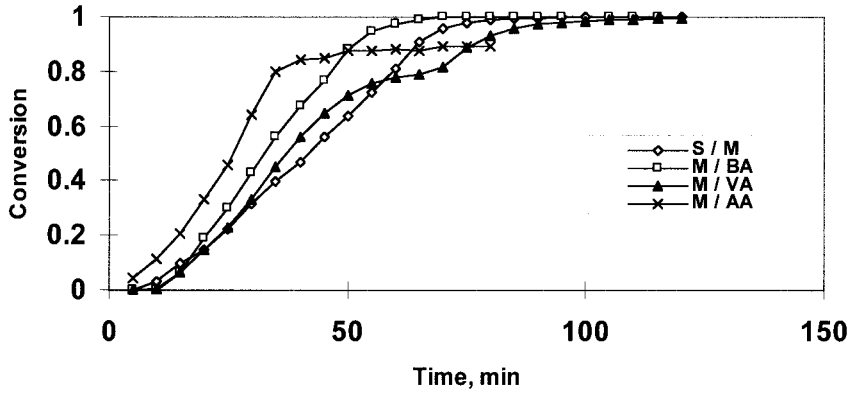

Figure 12 Conversion versus time curves for the copolymers of methyl methacrylate M/S, M/BA, M/AA, M/VA (70%/30%): T = 60°C, I = 0.45 g/L H_2O, E = 4 g/L H_2O, M_T = 0.34 g/cm^3 H_2O.

should be close to one. In this case it is obvious that one can predict the compositions without knowing the partitioning coefficients. On the other hand, for systems such as S/AA, with one monomer with low water solubility and one with high water solubility, the ratio of partitioning coefficients will be different from one, so that stronger influence of monomer partitioning would be expected. The system S/AA was the only one not simulated by the partition model, due to the full solubility of AA in water. However, even for this system with large differences in water solubility of the two comonomers, the simple approach using global compositions seems satisfactory, as shown in Figure 16.

Besides experimental and analytical errors, there may exist other causes of deviation between the model results and the experimental data, e.g., there is some variation in the values of reactivity ratios taken from different sources in the literature. Even the adjustment of reactivity ratios would lead to better agreement, but such an artificial compensation would disguise the role of monomer partition (phase equilibrium). While the monomer partition is not crucial for the calculation of copolymer composition as a function of global monomer conversion, even for monomers with different solubility in water, as shown by our results, it might be important to correctly predict the polymerization rate (and conversion versus time curves). The polymerization rate prediction is more complex as it depends on total sorbed monomer concentration, monomer partition ratio, rate constants, as well as reactivity ratios, and other phenomena like radical desorption. These

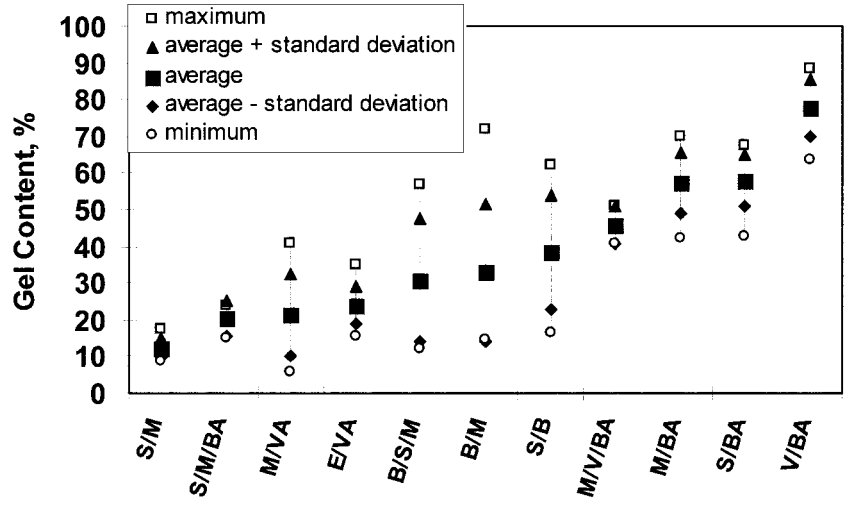

Figure 13 Gel content for each of the studied systems.

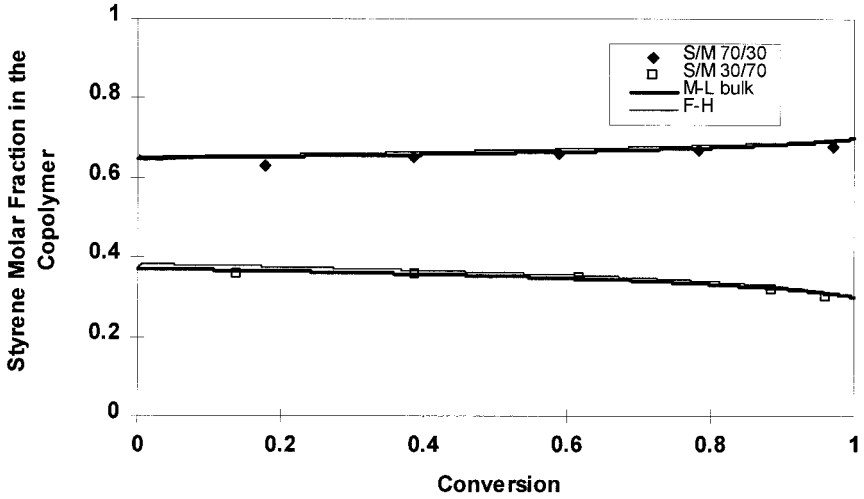

Figure 14 Polymer composition (mol % in PS) vs conversion for the system S/M, for two initial composition of S (70 and 30%): $T = 60°C$, $I = 0.45$ g/L H_2O, $E = 4$ g/L H_2O, $M_T = 0.34$ g/cm^3 H_2O. Solid lines are simple model simulations considering global monomer composition. Dashed lines are model simulations accounting for monomer partitioning.

considerations will be further discussed in the second paper of this series.

Average Number of Radicals per Particle

The average number of radicals per particle was evaluated for each system from the experimental data of monomer conversion, particle diameter, and estimated monomer and polymer composition, as follows:

$$\bar{n} = \frac{R_p \cdot N_A}{\bar{k}_p \cdot M_p \cdot N_p} \tag{8}$$

where $\bar{n}$ is the average number of radicals per particle (radicals/particle), R_p is the polymerization rate (mol/cm^3 of water/s), N_A is the Avogadro number, M_p is the concentration of monomers in the particles (mol/L of particle), k_p is the propagation rate constant (L/mol · s), and N_p is the

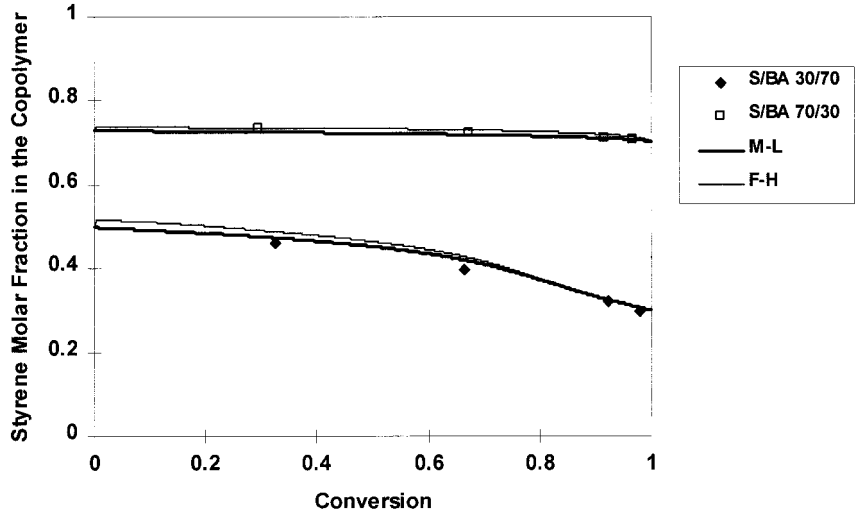

Figure 15 Polymer composition (mol % in PS) vs conversion for the system S/BA, for two initial composition of S (70 and 30%): $T = 70°C$, $I = 0.45$ g/L H_2O, $E = 4$ g/L H_2O, $M_T = 0.34$ g/cm^3 H_2O. Solid lines are simple model simulations considering global monomer composition. Dashed lines are model simulations accounting for monomer partitioning.

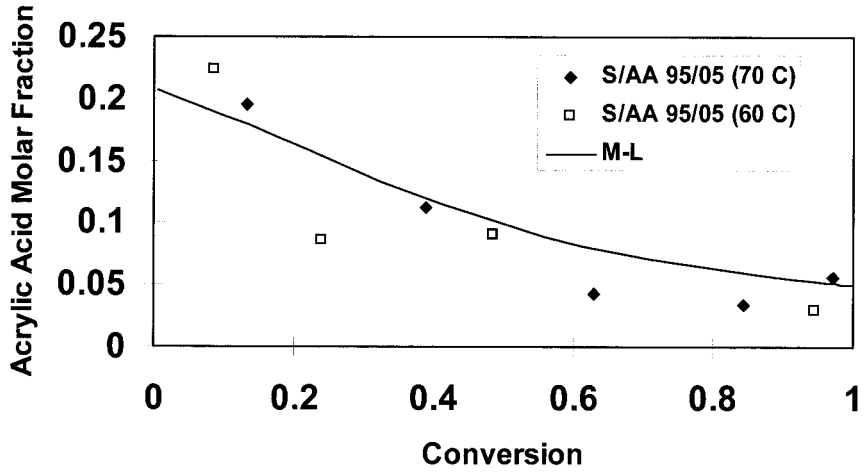

Figure 16 Polymer composition (mol % in PAA) vs conversion for the system S/AA, initial composition of AA = 5%: T = 60 and 70°C, I = 0.45 g/L H_2O, E = 4 g/L H_2O, M_T = 0.34 g/cm^3 H_2O. Solid lines are simple model simulations considering global monomer composition.

number of particles per unit volume of water (particles/cm^3 of water).

Polymerization rates were obtained by fitting a smoothed polynomial function to the conversion vs time data. The pseudo-homopolymerization rate constant of propagation is given by

$$\overline{k_p} = (k_{11} \cdot f_1 + k_{12} \cdot f_2) \cdot \varphi_1 + (k_{22} \cdot f_2 + k_{21} \cdot f_1) \cdot \varphi_2 \quad (9)$$

where f_i is the mole fraction of monomer i in the monomer mixture in the particles; k_{ab} is the propagation rate constant of radical type a with monomer type b (cm^3/mol/s).

The mole fraction of free radicals of type 1 and type 2 in the particles φ_i were calculated by

$$\varphi_1 = \frac{k_{21} \cdot f_1}{k_{21} \cdot f_1 + k_{12} \cdot f_2} \quad (10)$$

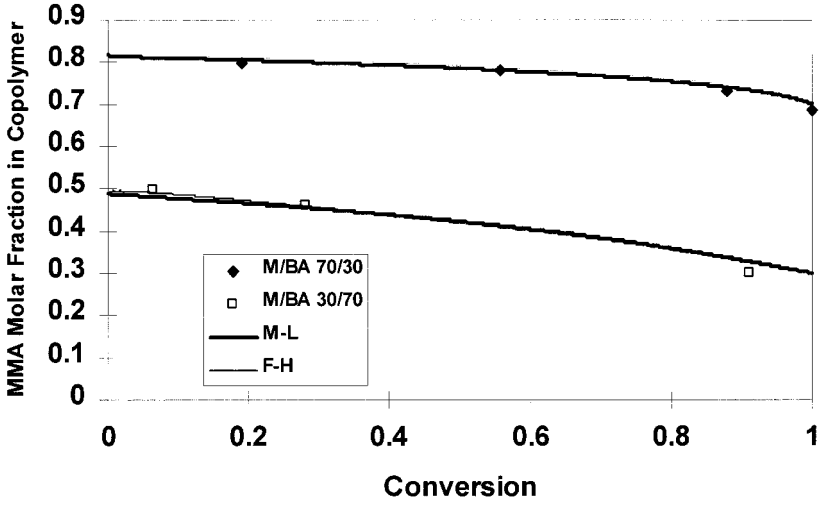

Figure 17 Polymer composition (mol % in PM) vs conversion for the system M/BA, for two initial composition of M (70 and 30%): T = 60°C, I = 0.45 g/L H_2O, E = 4 g/L H_2O, M_T = 0.34 g/cm^3 H_2O. Solid lines are simple model simulations considering global monomer composition. Dashed lines are model simulations accounting for monomer partitioning.

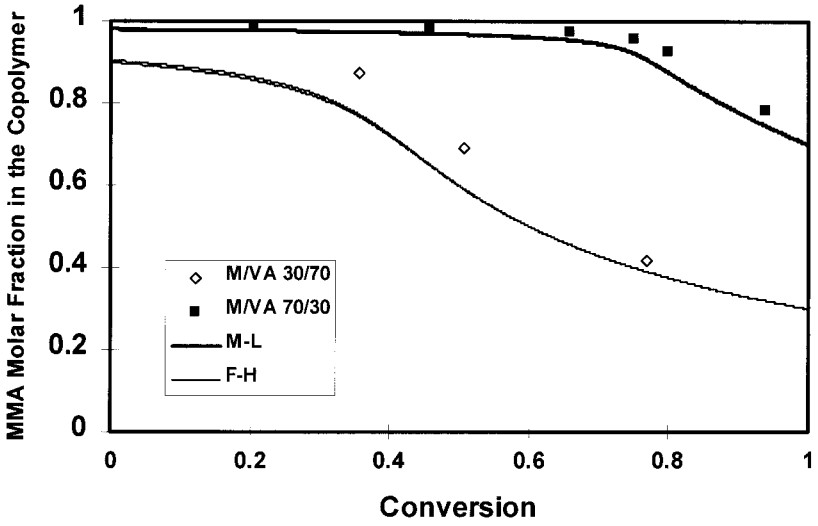

Figure 18 Polymer composition (mol % in PM) vs conversion for the system M/VA, for two initial composition of M (70 and 30%): T = 60°C, I = 0.45 g/L H_2O, E = 8 g/L H_2O, M_T = 0.34 g/cm^3 H_2O. Solid lines are simple model simulations considering global monomer composition. Dashed lines are model simulations accounting for monomer partitioning.

$$\varphi_2 = 1 - \varphi_1 \tag{11}$$

The mole fractions of monomer i in the particle f_i were first approximated by the total mole fractions of unreacted monomer i in the reactor, f_i' as discussed earlier, using eq. (5).

Finally, the concentration of monomers in the particles was obtained as follows:

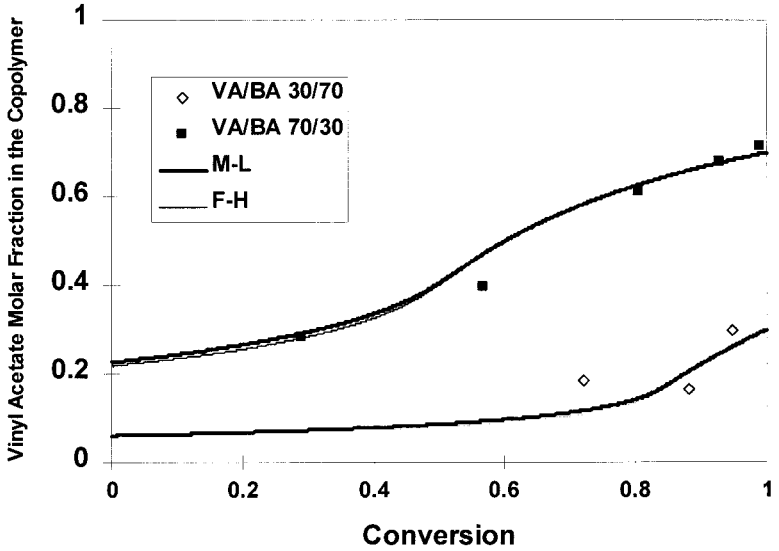

Figure 19 Polymer composition (mol % in PVA) vs conversion for the system VA/BA, for two initial composition of VA (70 and 30%): T = 70°C, I = 0.45 g/L H_2O, E = 4 g/L H_2O, M_T = 0.34 g/cm^3 H_2O. Solid lines are simple model simulations considering global monomer composition. Dashed lines are model simulations accounting for monomer partitioning.

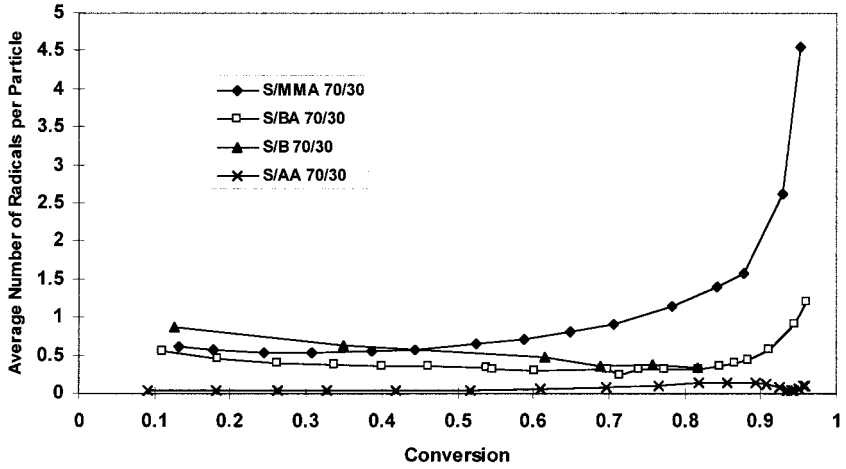

Figure 20 Average number of radicals per particle for the systems with 70 mol % of styrene in the initial monomer composition: $T = 60°C$, $M_T = 0.34$ g/g of water, $E = 4$ g/L of water, $I = 0.45$ g/L of water.

$$M_p = \frac{(1 - x_m)}{(x_m/\rho_p + (1 - x_m)/\rho_m) \cdot (f_1 \cdot MW_1 + f_2 \cdot MW_2)} \quad (12)$$

where x_m is the fractional weight conversion, ρ_p is the polymer density (g/cm3), ρ_m is the density of monomer mixture (g/cm^3), and MW_i is the molecular weight of monomer i. Equation (11) assumes that monomer droplets are not present; therefore, is not exactly valid for intervals I and II. Comparison between the results from the two approaches discussed in the section "Copolymer Composition" have shown that the error introduced by eq. (12) was only significant at global monomer conversions below 25%, and even in this range, the deviation introduced was not higher than 20%. In addition, for most of the systems studied, the droplets disappear (or strongly decrease) at about 20–25% conversion. Therefore, errors introduced by eq. (12) only affects the calculation for low conversions.

The results for the average number of radicals per particle are presented in Figures 20 and 21. Figure 20 shows the results for copolymerization

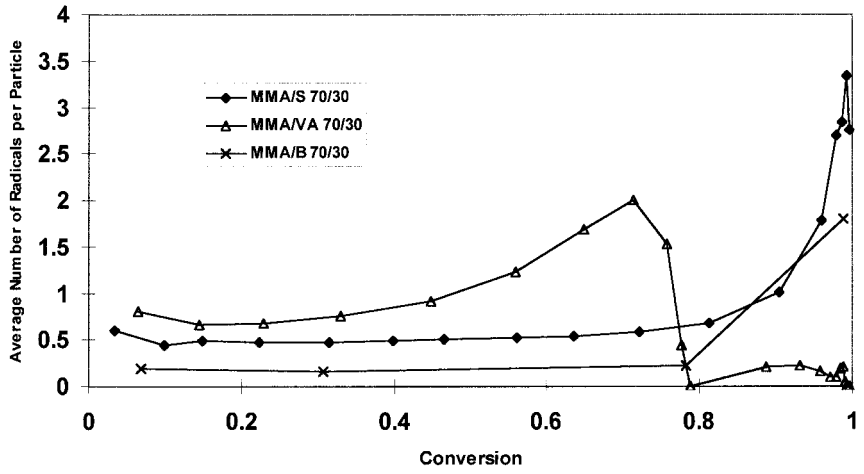

Figure 21 Average number of radicals per particle for the systems with 70 mol % of methyl methacrylate in the initial monomer composition: $T = 60°C$, $M_T = 0.34$ g/g of water, $E = 4$ g/L of water, $I = 0.45$ g/L of water.

runs with 70% styrene. The system S/MMA nearly follows Smith–Ewart case II kinetics ($\bar{n} = 0.5$) up to about 60% conversion; for higher conversions $\bar{n}$ increases reflecting the "gel" effect (Trommsdorff–Norrish effect) for this system. The gel effect is much less pronounced for the system S/BA, and the system S/B did not present any significant increase in n for high conversions. Systems S/BA and S/B also behave close to Smith–Ewart case II kinetics. On the other hand, the values of $\bar{n}$ observed for the system S/AA were much lower than 0.5 (Smith–Ewart case I kinetics). Radical desorption and termination in aqueous phase are not negligible in the system with acrylic acid. Another factor in this case is the higher rate of homogeneous nucleation.

Figure 21 shows the results for systems with 70% MMA. The system MMA(70)/S(30) behaves quite similar to the system MMA(30)/S(70) shown in Figure 20. The system MMA/VA shows the interesting feature of two consecutive homopolymerizations. Up to about 70% conversion the behavior is that of a Smith–Ewart case II kinetics with gel effect characteristic of MMA homopolymerization, and thereafter a strong change to a Smith–Ewart case 1 kinetics of VA homopolymerization (which presents high transfer to monomer).

CONCLUDING REMARKS

An extensive experimental study of batch co- and terpolymerization was carried out using several industrially important monomers. The experimental planning allowed for a systematic study of the effect of different monomer types and process conditions on the polymer quality and productivity. The monomers studied cover a wide range of monomer solubility in water and reactivity ratios. The experimental results and their discussion may improve our knowledge about the process and provide a large data bank for supporting mathematical modeling efforts. This will be further explored in the subsequent papers of this series. In this Part I we restrict ourselves to a more qualitative and comparative discussion of the global results.

The classic copolymerization equation was tested using the global monomer composition rather than the monomer concentration into the particles. It was found that this simple approach represented well the experimentally measured copolymer composition for several systems. This was further checked by verifying the close agreement of these results from this simplified approach with those from a more accurate model accounting for the monomer partitioning. Significant deviations between predictions and real data were found only for those pairs involving monomers with different water solubilities, especially in cases with higher amount of high water-soluble monomer. This is an indication that the monomer partitioning plays a role only in the cases of high soluble comonomers. While the monomer partition is not crucial for the calculation of copolymer composition as a function of global monomer conversion, even for monomers with different solubility in water, it might be important to correctly predict the polymerization rate. The polymerization rate prediction is more complex as it depends on total sorbed monomer concentration, monomer partitioning, rate constants, as well as reactivity ratios, and other phenomena like radical desorption. These considerations will be further discussed in Part II of this series.

The presence of gel was studied and quantified in an approximated way by measuring the residue when filtering the polymer. Such approximated technique enabled us for a qualitative and comparative study. The gel content was higher in copolymers and terpolymers involving acrylic acid, butyl acrylate, and butadiene. The increase in M concentration causes a reduction in the gel content.

The number of particles was higher for the systems with acrylic acid and butadiene. The effect of AA can be attributed to the intensification of homogeneous nucleation, and also to the enhancement of particle stabilization by the emulsification action of this monomer.

The average number of radicals per particle estimated from the data can bring important knowledge about the importance of desorption and termination in aqueous phase in the polymerization processes that have been studied.

The authors are grateful to CNPq, FAPESP, Rhodia, CID-GIRSA, and UWPREL for support of this work.

REFERENCES

1. Mayo, F. R.; Lewis, F. M. J Am Chem Soc 1944, 66, 1594.
2. Alfrey, T., Jr.; Goldfinger, G. J Chem Phys 1944, 12, 115, 205, 332.
3. Ma, Y.; Won, Y.; Kubo, K.; Fukuda, T. Macromolecules 1993, 26, 6766.

4. Fukuda, T.; Ma, Y.; Inagaki, H. Macromolecules 1985, 18, 17.
5. Melville, H. W.; Noble, B.; Watson, W. F. J Polym Sci 1947, 2(2), 229.
6. Dougherty, E. J Appl Polym Sci 1986, 32, 3051.
7. Brandrup, J.; Immergut, E. H. Polymer Handbook, 3rd ed.; Wiley—Interscience: New York, 1989.
8. Min, K. W. Ph.D. thesis, State University of New York at Buffalo, 1976.
9. Saldívar, E.; Dafniotis, P.; Ray, W. H. JMS—Rev Macromol Chem Phys 1998, C38(2), 207.
10. Penlidis, A. Can J Chem Eng 1994, 72, 385.
11. Box, G. E. P.; Hunter, W. G.; Hunter, J. S. Statistics for Experimenters; Wiley: New York, 1978.
12. Walas, S. M. Phase Equilibrium in Chemical Engineering; Butterworth-Heinemann, 1985.
13. Araujo, O. Ph.D. Thesis (in Portuguese), Polytechnic School University of Sao Paulo, Brazil, 1997.
14. Weertz, P. A.; German, A. L.; Gilbert, R. G. R. G. Macromolecules 1991, 24, 1622.
15. Dubé, M. A.; Penlidis, A. Polym Intl 1995, 37, 235.
16. Saldívar, E.; Ray, W. H. AIChE J 1997, 43(8), 2021.
17. Odian, G. Principles of Polymerization, 3rd ed.; Wiley: New York, 1991.
18. Charmot, D.; Guillot, J. Polymer 1992, 33(2), 353.
19. Gao, J.; Penlidis, A. JMS—Rev Macromol Chem Phys 1996, C36(2), 199.
20. Gugliotta, L. M.; Arzamendi, G.; Asua, J. M. J Appl Polym Sci 1995, 55, 1017.
21. Armitage, P. D.; de la Cal, J. C.; Asua, J. M. I J Appl Polym Sci 1994, 51, 1985.